Phase Behavior of Ternary Homopolymer/Diblock Blends: Influence of Relative Chain Lengths

Philipp K. Janert* and M. Schick

Department of Physics, Box 351560, University of Washington, Seattle, Washington 98195-1560

Received July 19, 1996; Revised Manuscript Received November 4, 1996[⊗]

ABSTRACT: We study the phase behavior of ternary blends of A- and B-homopolymers and symmetric, or slightly asymmetric, AB-diblock copolymer as obtained from self-consistent field theory. We choose one value of the segregation in the weak to intermediate regime and determine the effects of varying the relative degrees of polymerization of the components. The diagrams we obtain, which contain the classical lyotropic phases, exemplify and make concrete a few general principles. Homopolymers longer than the diblocks are expelled from the microstructure, while homopolymers of comparable length swell the microstructure, a swelling which can proceed indefinitely. Very short homopolymers disorder the microstructure. Our results can be understood as due to the varying ability of homopolymers of different length to swell the brush formed by the diblock at the internal interfaces.

I. Introduction

Systems containing block copolymers are interesting due to their ability to cause ordered phases of various symmetries to form spontaneously.[1] Besides being of both fundamental and applied interest in their own right, polymer mixtures provide systems which are well-characterized, both experimentally and theoretically, with which to study the phenomenon of self-assembly, a phenomenon also displayed by lipids and short-chain surfactants.

The behavior of a melt of pure AB-diblock is rather well-understood.[2,3] At sufficiently small values of the effective interaction parameter χN, where χ is the dimensionless incompatibility between unlike segments and N is the number of statistical segments per chain, the melt is disordered. As χN is increased, either by lowering the temperature or by increasing the chain length, the incompatibility causes the system to order. Because of the connectivity of the blocks, there can be no macroscopic phase separation into two phases of like components. Instead, the melt undergoes a microphase separation characterized by extensive amounts of internal interface which separate coherent regions of A-monomer from B. The copolymer chains straddle the interfaces, forming a "brush" on either side. The symmetry of the ordered phase is determined by the architecture of the diblock, that is, the fraction f of it which is comprised of A-monomer. In an almost symmetric diblock, the cost to stretch either block is nearly the same, with the consequence that the system forms the flat interfaces of lamellar phases. However, if one of the blocks is sufficiently longer than the other, a curved interface is formed, with the longer block on the outside. This allows the longer block to relax, which more than compensates for the necessary stretching of the shorter block on the inside of the curved interface.

Our understanding of blends containing diblock copolymer is far less complete, although much progress has been made recently.[4,5] The simplest system consists of an AB-diblock blended with A-homopolymer, of chain lengths N and N_A, respectively. The fact that this system is now a true two-component mixture permits two behaviors absent in the pure diblock case. On the one hand, the blend can phase-separate into two distinct bulk phases, each of which can be microstructured. On the other, the blend can be swollen by added homopolymer. In the extreme case, this swelling can proceed indefinitely so that the period of the microstructure grows without limit. This leads to the complete unbinding of the ordered phase.[5−7] These additional behaviors take place in the enlarged parameter space of the binary blend which comprises not only the polymerization index N and fraction f of the diblock, but also the volume fraction ϕ of the homopolymer and its chain length $N_A = \alpha_A N$. The topology of the phase diagram is largely determined by the parameter α_A.

As noted above, the spontaneous curvature of a copolymer layer is determined by the composition parameter f. The ability of A-homopolymer chains to enter a diblock layer is determined by the relative chain lengths, i.e. by α_A. This ability has been studied in systems of polymers grafted at one end to a surface and immersed in a homopolymer melt. It was found[8] that homopolymers longer than the chains in the brush are expelled from it ("dry" brush), while those which are shorter swell the brush ("wet" brush). This argument was later extended to several other situations: to brushes formed by diblocks assembled at an internal flat interface between coexisting bulk phases of immiscible homopolymers, to the curved interfaces of copolymer micelles,[9,10] and to the phase behavior of binary homopolymer/diblock blends in the strong segregation limit.[11]

Phase diagrams for the case of binary AB/A blends have recently been calculated[5] and are generally in good agreement with experiment. Our aim is to extend such calculations to ternary systems of AB-diblocks which are blended with both A- and B-homopolymer.

Our motivation is 3-fold: First, the microphase separation behavior of ternary blends has received little experimental attention.[12−16] Theoretical studies have concentrated either on the interfacial activity of diblock copolymers between coexisting bulk phases[17,18] or on the phase diagram of disordered, homogeneous phases.[19,20] The only theoretical study[21] focusing specifically on the microphase behavior of ternary blends was severely restricted by approximations made in addition to that of the mean-field theory. In particular, the restriction to the lamellar phase as the only ordered structure and

[⊗] Abstract published in *Advance ACS Abstracts,* December 15, 1996.

S0024-9297(96)01068-6 CCC: $14.00

its description by a single Fourier component caused some crucial features to be missed, e.g. the complete unbinding. Thus our primary goal is to elucidate the general phase behavior of these important systems, particularly with regard to the lyotropic phases.

The parameter space of the ternary system A/B/AB is rather large, as there are two independent chain length ratios and two independently variable volume fractions, in addition to f and χN. The dependence of the phase behavior on these parameters is not obvious, and determining it experimentally is not practical. Thus, our second goal is to produce a representative catalogue of typical phase diagrams and to give physically motivated interpretations of them that permit the extension of our results to related systems.

Lastly, it is of interest to make possible the comparison of ternary homopolymer/diblock melts with water, oil, and surfactant systems for which an enormous number of experimental phase diagrams has been assembled.[22,23] The apparently universal character of self-assembly as manifested in the often observed sequence of lamellar to hexagonal to body-centered-cubic to disordered phases with increasing dilution of the amphiphile leads one to expect that information about short-chain amphiphiles can be gained from the study of polymers. The latter are far more easily described theoretically than the former. Of course with the synthesis of long chain surfactants,[24] the distinction between the two systems is becoming increasingly artificial.

Our paper is organized as follows. In the next section, we develop the self-consistent field theory of the AB/A/B system in the grand canonical ensemble and in a Fourier representation. In section III, we present the phase diagrams obtained and interpret their structure using arguments based upon wet and dry brushes. In the final section, we summarize our main arguments as to the dependence of the phase behavior on the parameters of the system and conclude with a few additional observations.

II. Theory

We consider a ternary blend of A- and B-homopolymer, of polymerization indices $\alpha_A N$ and $\alpha_B N$, respectively, and AB-diblock of index N of which a fraction f is A-monomer. We employ the Gaussian model of flexible polymer chains and work in the grand canonical ensemble in which the number n_κ of chains of type $\kappa =$ A, B, AB is not fixed.[4] The configurational part of the partition function is

$$Z \propto \sum_{n_A}^{\infty}\sum_{n_B}^{\infty}\sum_{n_{AB}}^{\infty} \frac{z_0^{n_{AB}}(z_A z_0)^{n_A}(z_B z_0)^{n_B}}{n_{AB}!n_A!n_B!} \int\prod_{i=1}^{n_A}\tilde{D}\mathbf{r}_{A,i}\prod_{j=1}^{n_B}\tilde{D}\mathbf{r}_{B,j}\prod_{k=1}^{n_{AB}}\tilde{D}\mathbf{r}_{AB,k}\exp\left[-\chi\int\frac{d\mathbf{r}}{v}\hat{\Phi}_A(\mathbf{r})\hat{\Phi}_B(\mathbf{r})\right] \tag{2.1}$$

where v is the volume occupied by each monomer, $z_\kappa = \exp(\beta\mu_\kappa)$, $\beta = 1/k_B T$, and μ_κ is the chemical potential of component κ to within an additive constant z_0. Tildes indicate that the functional integrals are weighted by the Wiener measure $P[\mathbf{r};0,1]$ for diblocks and $P[\mathbf{r};0,\alpha_A]$, $P[\mathbf{r};0,\alpha_B]$ for the homopolymers, where

$$P[\mathbf{r};0,s_0] \propto \exp\left(-\frac{3}{2Na^2}\int_0^{s_0} dt\left|\frac{d\mathbf{r}}{dt}\right|^2\right) \tag{2.2}$$

where a is the statistical segment length taken to be the same for both monomers. To simplify the formulae below, we shall set $z_0 = Nv$.

Information about the configurations of the chains is contained in the local, dimensionless, densities. That of the A-monomers is

$$\hat{\Phi}_A(\mathbf{r}) = \hat{\Phi}_A(\mathbf{r},\{\mathbf{r}_{A,i}\},\{\mathbf{r}_{AB,k}\}) \tag{2.3}$$

$$= Nv\sum_i^{n_A}\int_0^{\alpha_A} ds\ \delta(\mathbf{r}-\mathbf{r}_{A,i}(s)) + Nv\sum_k^{n_{AB}}\int_0^{f} ds\ \delta(\mathbf{r}-\mathbf{r}_{AB,k}(s)) \tag{2.4}$$

A similar expression holds for $\hat{\Phi}_B$. We include a hard core repulsion between monomers by requiring the melt to be incompressible. As a consequence, there are only two independent chemical potentials, and we set that of the copolymer to zero.

To make the expression for the partition function more tractable, one inserts a functional integral $1 = \int D\Phi_A D\Phi_B \delta[\Phi_A-\hat{\Phi}_A]\delta[\Phi_B-\hat{\Phi}_B]$, which permits the replacement of the densities $\hat{\Phi}_A$ and $\hat{\Phi}_B$, which depend on the polymer configurations, by the functions Φ_A and Φ_B, which do not. After inserting a standard representation for the δ-function $\delta[\Phi_A-\hat{\Phi}_A] = \int DW_A \exp[W_A-(\Phi_A-\hat{\Phi}_A)]$, where W_A is imaginary, and similarly for the other δ-function and carrying out the summations over n_κ, we arrive at the following form of the partition function

$$Z \propto \int D\Phi_A D\Phi_B DW_A DW_B \exp(-\beta F[\Phi_A,\Phi_B,W_A,W_B]), \tag{2.5}$$

where the free energy functional is:

$$-Nv\beta F[\Phi_A,\Phi_B,W_A,W_B] = z_A Q_A[W_A] + z_B Q_B[W_B] + Q_{AB}[W_A,W_B] + \int d\mathbf{r}[\Phi_A(\mathbf{r})\ W_A(\mathbf{r}) + \Phi_B(\mathbf{r})\ W_B(\mathbf{r}) - \chi N\Phi_A(\mathbf{r})\ \Phi_B(\mathbf{r})] \tag{2.6}$$

The Q_κ are the partition functions of *single* polymers in external fields W_A and/or W_B. These single polymer partition functions can be obtained from $Q_\kappa = \int d\mathbf{r}\ q_\kappa(\mathbf{r},\alpha_\kappa)$, $\kappa =$ A, B, and $Q_{AB} = \int d\mathbf{r}\ q_{AB}(\mathbf{r},1)$ where the end-segment distribution functions are

$$q_\kappa(\mathbf{r},s_0) = \int D\mathbf{r}_\kappa P[\mathbf{r}_\kappa;0,s_0]\delta(\mathbf{r}-\mathbf{r}_\kappa(s_0)) \exp\left(-\int_0^{s_0} ds\int\frac{d\mathbf{r}}{v}w_\kappa\hat{\Phi}_\kappa\right) \qquad \kappa = \text{A, B} \tag{2.7}$$

$$q_{AB}(\mathbf{r},s_0) = \int D\mathbf{r}_{AB} P[\mathbf{r}_{AB};0,s_0]\delta(\mathbf{r}-\mathbf{r}_{AB}(s_0)) \exp\left(-\int_0^{s_0} ds\int\frac{d\mathbf{r}}{v}[w_A\hat{\Phi}_A + w_B\hat{\Phi}_B]\right) \tag{2.8}$$

Because the polymers are modeled as Gaussian chains, these distributions satisfy the diffusion equations

$$\frac{\partial q_{AB}}{\partial s} = \begin{cases}\dfrac{Na^2}{6}\nabla^2 q_{AB} - W_A q_{AB} & s < f\\ \dfrac{Na^2}{6}\nabla^2 q_{AB} - W_B q_{AB} & s > f\end{cases} \tag{2.9}$$

for the diblock and

$$\frac{\partial q_\kappa}{\partial s} = \frac{Na^2}{6}\nabla^2 q_\kappa - W_\kappa q_\kappa \qquad \kappa = \text{A, B} \quad (2.10)$$

for the homopolymers, respectively. The initial conditions are $q_\kappa(\mathbf{r},0) = 1$ for all components. Because the two ends of the diblock are distinct, it is also necessary to introduce $q^\dagger_{AB}(\mathbf{r},s)$, which is defined similiarily to q_{AB}, except that the functional integral eq 2.8 is taken from s_0 to 1. It satisfies (2.9) with the left-hand side multiplied by -1 and with the initial condition $q^\dagger_{AB}(\mathbf{r},1) = 1$.

In place of calculating the exact free energy, the self-consistent field theory approximates it by the value of the free energy functional $F(\Phi_A,\Phi_B,W_A,W_B)$ obtained by extremizing it under the incompressibility constraint, which is incorporated by means of Langrange multiplier ξ. The densities and fields which extremize the free energy, and which we denote by ϕ_A, ϕ_B, w_A, and w_B are solutions of the variational equations

$$\phi_A = z_A\frac{\delta Q_A[w_A]}{\delta w_A} + \frac{\delta Q_{AB}[w_A,w_B]}{\delta w_A} \quad (2.11)$$

$$\phi_B = z_B\frac{\delta Q_B[w_B]}{\delta w_B} + \frac{\delta Q_{AB}[w_A,w_B]}{\delta w_B} \quad (2.12)$$

$$w_A = \chi N\phi_A + \xi \quad (2.13)$$

$$w_B = \chi N\phi_B + \xi \quad (2.14)$$

$$1 = \phi_A + \phi_B \quad (2.15)$$

From eqs 2.11 and 2.15 and the definition of the single polymer partition functions Q_κ, it is seen that ϕ_A is the ensemble average of $\hat{\Phi}_A$, and similarly for ϕ_B. They can be written in terms of the end-segment distribution functions as

$$\phi_A = z_A\int_0^{\alpha_A} \mathrm{d}s\; q_A(\mathbf{r},s)\, q_A(\mathbf{r},\alpha_A - s) + \int_0^f \mathrm{d}s\; q_{AB}(\mathbf{r},s)\, q^\dagger_{AB}(\mathbf{r},s) \quad (2.16)$$

A similar expression holds for ϕ_B.

We now expand all functions of position in a complete set of orthonormal eigenfunctions of the Laplacian which possess the symmetry of the phase being considered. This converts eqs 2.9−2.15 between functions into a discrete set of coupled equations for the Fourier coefficients. Upon truncation of the eigenfunction expansion, the equations are solved exactly following ref 25. The number of basis functions retained determines the accuracy of the solution. The maximum number that we can handle computationally is 50. The basis functions contain a length scale D of the ordered structure, and the free energy is minimized with respect to it. By comparing the value of the free energy for different phases, one constructs the phase diagram. In addition to the disordered (DIS) phases, we are interested in the general behavior of the lyotropic ones. We consider only the simple, "classical" ones: sheet-like lamellae (LAM); cylinders, arranged on a hexagonal lattice (HEX); and spheres, arranged on a body-centered-cubic lattice (BCC). It is known that most of the other phases which could arise, such as the gyroid and the hexagonally perforated lamellar phase,[26,27] would be located in a narrow region between the lamellar and cylindrical phases.

Density profiles of strongly swollen phases are far from sinusoidal and require a large number of basis functions to be represented well. However, we find that the value of the free energy is relatively insensitive to the number of terms kept. Additionally, we find that for strongly swollen phases, the minimum of the free energy as a function of D is extremely broad, so that phases with very different length scales and compositions are nearly equal in free energy. Since the composition of a phase is calculated with far less accuracy than its free energy, we draw the boundaries of strongly swollen phases with dashed lines in all figures.

III. Results and Discussion

In Figures 1−11, we present constant temperature cuts through the three-component phase prism for eleven different systems of a diblock copolymer and corresponding homopolymers.

As explained above, the parameter space of the general three-component system is too large to be mapped out completely. We restrict ourselves therefore to one value of the interaction parameter, $\chi N = 11.0$, and, with one exception shown in Figure 11, to a symmetric diblock, $f = 0.5$. This way we retain the feature characteristic of ternary blends, namely the competition between the two homopolymers, in general of unequal length, to swell the brush formed by the diblock at the internal interface. We elucidate this behavior by systematically varying α_A and α_B. We discuss the influence of changing f and χN in Figure 11 and further below.

The diagrams in Figures 1−10 are divided into two sequences. In Figures 1−6, the A-homopolymer is shorter than the diblock and its relative length is kept fixed at $\alpha_A = 0.3$, while that of the B-homopolymer varies from $\alpha_B = 1.2$ to 0.1. In the second sequence, Figures 7−10, the B-homopolymer is longer than the diblock and of fixed length $\alpha_B = 1.5$, while that of the A-homopolymer varies from $\alpha_A = 1.5$ to 0.5.

We now discuss each phase diagram in turn. In Figure 1, we show the constant temperature phase diagram of a system with $\alpha_A = 0.3$ and $\alpha_B = 1.2$, in other words, the diblock is slightly shorter than the B-homopolymer, while it is about three times as long as the A-homopolymer. Regions of phase coexistence between an ordered and a disordered phase dominate the phase diagram. The B-homopolymer is, for the most part, expelled from the microstructure formed by the diblock and is found in a uniform, disordered phase of large B-homopolymer and very small A-homopolymer content that coexists with the diblock-rich, ordered phases. The volume fraction of B-homopolymer in the ordered phases does not exceed 0.25.

This result can be understood as follows. If the large B-homopolymer is added to an ordered microphase, it would preferentially assemble in the domains formed mainly by B-segments of the diblock so as to reduce the number of unfavorable A, B-contacts. However, since the size of those regions is comparable to the mean radius of gyration of the B-block, it is smaller than the size of the undisturbed B-homopolymer. Therefore, were a B-homopolymer to enter the microphase, it would have to be compressed. The loss of configurational entropy entailed by such an arrangement is large, whereas the gain of entropy of mixing is small because of the larger size of the homopolymer. On the other hand, the B-homopolymers, because of their relatively large length, lose little translational entropy by demix-

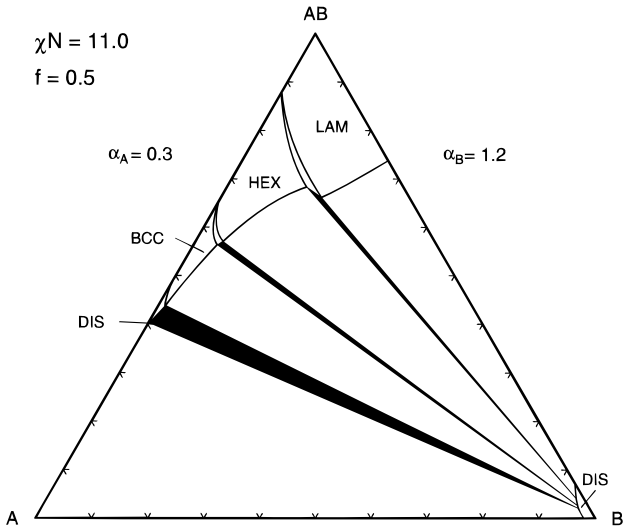

Figure 1. Constant temperature phase diagram of the ternary system of a symmetric AB-diblock copolymer of length N with an A-homopolymer of length $\alpha_A = 0.3N$ and a B-homopolymer of length $\alpha_B = 1.2N$. The value of the effective incompatibility parameter χN is 11.0. LAM denotes a lamellar phase; HEX, hexagonally arranged cylinders; BCC, spheres on a body-centered-cubic lattice; and DIS, homogeneous phases. Regions of three-phase coexistence are shaded, biphasic regions are unlabeled. Phase boundaries of strongly swollen phases, that could not be located exactly, are shown with dashed lines. Note the almost B-free disordered phase on the left hand side.

ing from the diblock copolymer. The net effect is that the B-homopolymer separates from the microstructure. For the same reasons, cylindrical and spherical domains accommodate less B-homopolymer than does the lamellar phase.

In contrast, the A-homopolymers, being considerably shorter than the A-block of the copolymer, are able to penetrate into the brush. In order to make room for the A-homopolymers and to avoid stretching the A-block of the copolymer, the layer of diblock bends with the convex side toward the A-homopolymers. This "wedge" effect of short homopolymers gives rise to a nonvanishing preferred curvature of the copolymer layer, even for symmetric diblocks. On the binary AB/A side, it brings about the ubiquitious sequence of first-order transitions toward phases with greater mean curvature of their internal interfaces: lamellar to hexagonal to body-centered-cubic. In addition to this wedge effect, the short homopolymer is able to reduce the stretching energy of the diblock chains in additional ways that favor this sequence of phases. Due to their relatively large translational entropy, the short A-homopolymer chains enter the cores of cylindrical and spherical structures thus relieving some of the stretching of the B-block. However this also increases the number of unfavorable A, B-contacts. They also enter the interstices between cylindrical and spherical structures, thus relieving the stresses induced by the inability of these units to fill space.

In the system shown in Figure 2, the B-homopolymer is now shorter than the diblock, but comparable to it, $\alpha_B = 0.9$. This leads to entirely different behavior on the AB/B binary side of the phase diagram. The B-homopolymer is no longer expelled from the microstructure, as it is not larger than the B-rich regions of the pure diblock phase. In fact, the B-domains of the lamellar phase accomodate any amount of B-homopolymer, which leads to a complete unbinding of the lamellar phase as the fraction of B-homopolymer is increased.

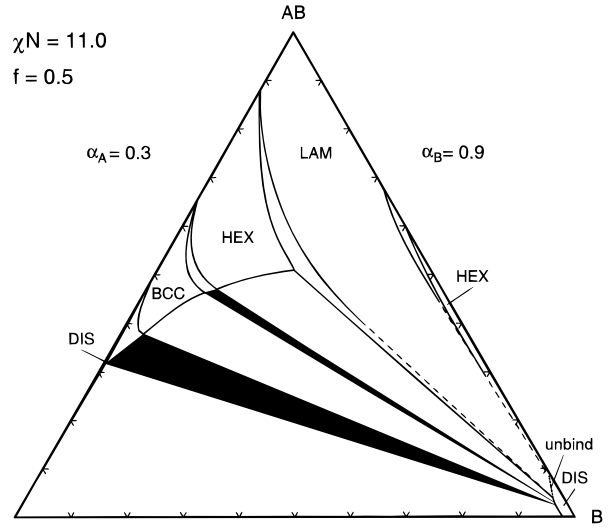

Figure 2. Phase diagram for a symmetric AB-diblock of length N with an A-homopolymer of length $\alpha_A = 0.3N$ and a B-homopolymer of length $\alpha_B = 0.9N$. The notation is that of Figure 1. Note the unbinding transition of the lamellar and hexagonal phases into the B-rich disordered phase.

The complete unbinding is a continuous transition, as the wavevector, characterizing the lamellar phase, vanishes without a jump. In this limit, the free energy density and the composition of the lamellar phase become equal to those of the disordered phase with the same chemical potential. This results from the fact that the slabs between lamellae become identical in composition to the disordered phase, and the lamellae, whose number per unit length vanishes, do not contribute an extensive term to the free energy. There is also a narrow region of A-cylinders in a B-matrix, brought about by the wedge effect of the B-homopolymers. The cylinders also unbind into the disordered phase on the B-rich side of the phase diagram.

On the A-rich side of the phase diagram, where B-blocks are in the center of cylinders and spheres, B-homopolymer cannot swell the B-blocks without changing the curvature of the internal interfaces, and this is prevented by the wedge effect of the short A-homopolymer. As a result, the phase boundaries of A-rich BCC and HEX phases change little from Figure 1 to Figure 2, in contrast to the major change in the lamellar phase boundary.

In the system shown in Figure 3, the B-homopolymer is now sufficiently short, $\alpha_B = 0.5$, to penetrate and swell the B-block of the copolymer. Therefore, the entire sequence of first-order transitions from lamellar to hexagonal to body-centered-cubic appears on the B-rich as well as on the A-rich side. As the homopolymers are of comparable length, the lamellar phase, in which the "wedge" effects of both homopolymer are balanced, occupies a large region of the phase diagram. Only when the lamellae are well-separated does the different ability of A- and B-homopolymers to swell the respective brushes becomes apparent, and a larger fraction of the longer B-homopolymer is necessary to balance the shorter A-homopolymer. In contrast to the situation in Figure 2 where the B homopolymers were too long to be incorporated into the cores of the cylindrical and spherical structures on the A-rich side of the diagram, the B-homopolymers are now short enough to enter the cylindrical or spherical structures and relieve some of the stretching energy of the diblock layer.

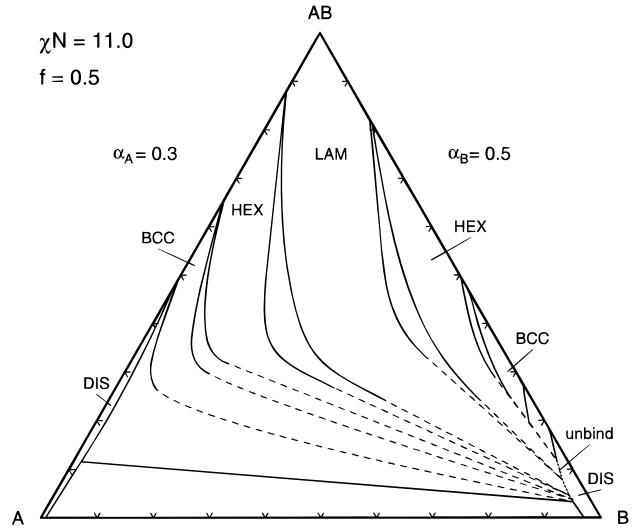

Figure 3. Phase diagram for a symmetric AB-diblock of length N with an A-homopolymer of length $\alpha_A = 0.3N$ and a B-homopolymer of length $\alpha_B = 0.5N$. The notation is that of Figure 1. Note the unbinding of strongly swollen ordered phases.

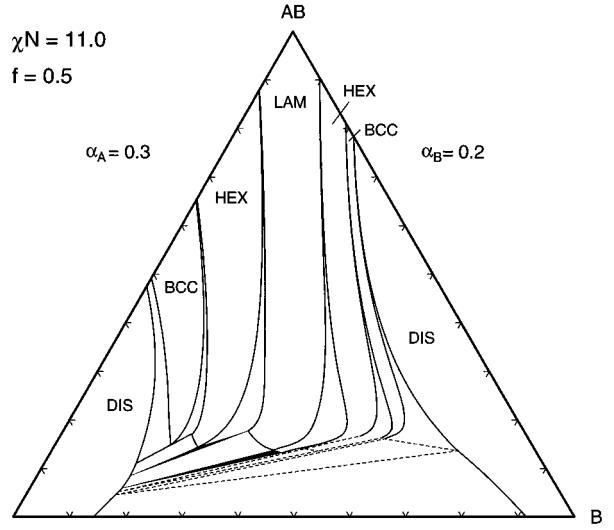

Figure 5. Phase diagram for a symmetric AB-diblock of length N with an A-homopolymer of length $\alpha_A = 0.3N$ and a B-homopolymer of length $\alpha_B = 0.2N$. The notation is that of Figure 1. Note the high copolymer concentration at the order/disorder transition on the right hand side.

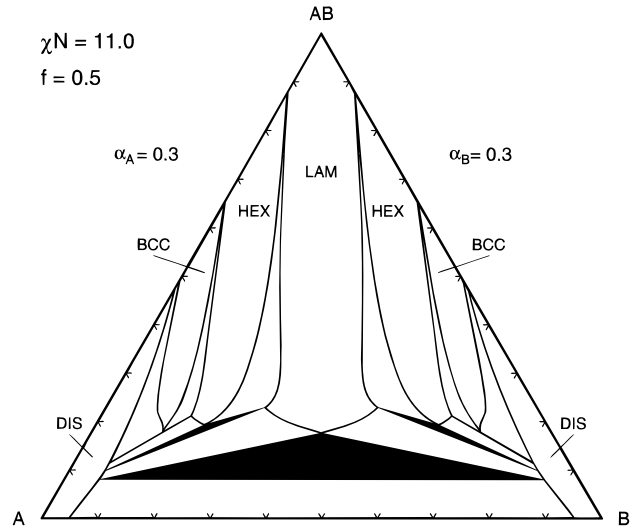

Figure 4. Phase diagram for a symmetric AB-diblock of length N with an A-homopolymer of length $\alpha_A = 0.3N$ and a B-homopolymer of length $\alpha_B = 0.3N$. The notation is that of Figure 1. Note the phase boundaries of the BCC phase for copolymer volume fraction smaller than 0.2 may be affected by truncation error (cf. text).

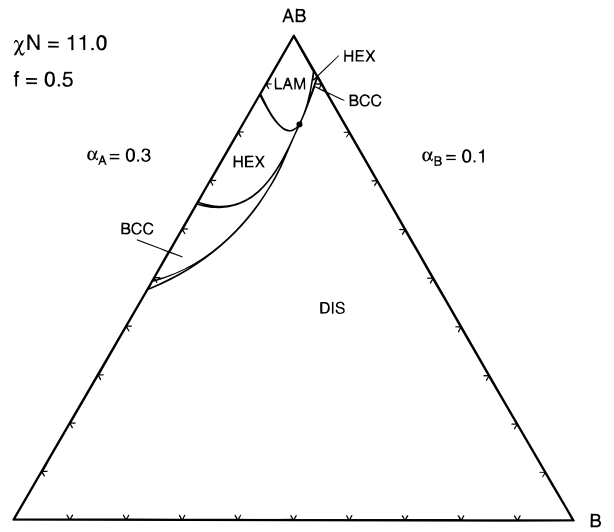

Figure 6. Phase diagram for a symmetric AB-diblock of length N with an A-homopolymer of length $\alpha_A = 0.3N$ and a B-homopolymer of length $\alpha_B = 0.1N$. The notation is that of Figure 1. The stability region of the B-rich BCC phase is too small to be resolved on the scale of this graph. The dot denotes Leibler's critical point. Note that the DIS/DIS demixing transition takes place at $\chi N = 12.44$ for this system.

The two homopolymers are of equal size in the system of Figure 4, with $\alpha_A = \alpha_B = 0.3$. A noteworthy feature is that while the ordered phases cannot be swollen very much on the binary sides of the diagram, even a small amount of the third component permits the structures to swell considerably. The reason is that on the A-rich side, for example, when A-homopolymers enter the B-cores to relieve stress, they also increase the number of unfavorable contacts. However the addition of B-homopolymer relieves the stress equally well without the enthalpic penality. Note also the absence of any unbinding transition. The homopolymers are now so short that the increase in translational entropy on forming a disordered phase outweighs the cost of increased A, B-contacts in such a phase.

We see the same trend continue in Figures 5 and 6. In Figure 5 the B-homopolymer chains are now quite short, $\alpha_B = 0.2$, and less than the value of 0.25 noted[19] to mark the onset of a disordering effect of added homopolymer. In accordance with this observation, the ordered phases on the B-rich side of the phase diagram can support no greater a volume fraction of B-homopolymer than $\phi_B = 0.21$, a small value compared with that on the A-rich side of $\phi_A = 0.54$ for only slightly longer chains. Note that, as in Figure 3 for well-separated lamellae, a larger number of longer chains are needed to balance the smaller chains. Otherwise, a transition to a hexagonal and then to a body-centered-cubic phase will occur with the longer homopolymer chains on the inside. This is again due to the stronger wedge effect of the shorter chains. Remarkably, this transition occurs for systems of Figures 3 and 5 at roughly the same lamellar spacing ($D \approx 2.5-3.0\ R_0$), although the diblock volume fraction is rather different.

In Figure 6, the last of this sequence, the length of the B-homopolymer is only $^1/_{10}$ that of the diblock.

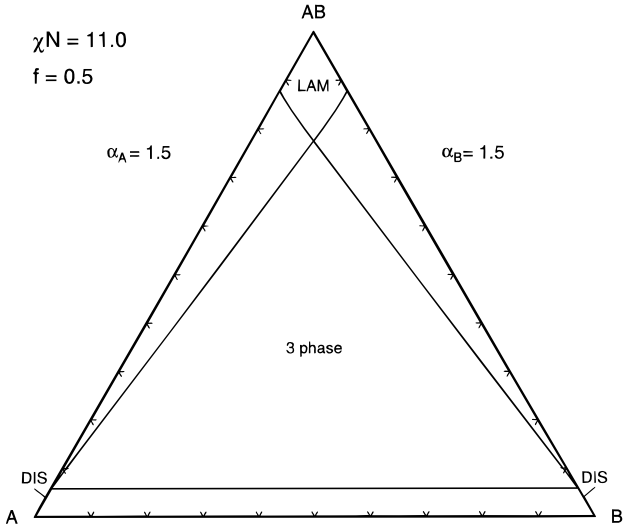

Figure 7. Phase diagram for a symmetric AB-diblock of length N with an A-homopolymer of length $\alpha_A = 1.5N$ and a B-homopolymer of length $\alpha_B = 1.5N$. The notation is that of Figure 1. Note the large region of three-phase coexistence between the lamellar and the A- and B-rich disordered phases.

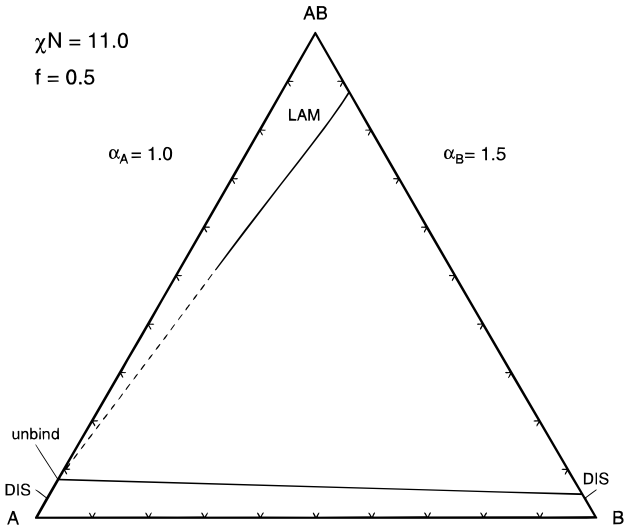

Figure 8. Phase diagram for a symmetric AB-diblock of length N with an A-homopolymer of length $\alpha_A = 1.0N$ and a B-homopolymer of length $\alpha_B = 1.5N$. The notation is that of Figure 1. The lamellar phase unbinds into the almost B-free disordered phase on the left hand side.

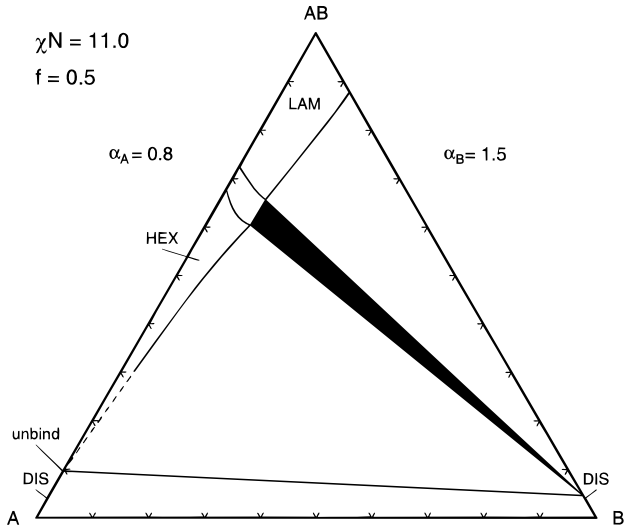

Figure 9. Phase diagram for a symmetric AB-diblock of length N with an A-homopolymer of length $\alpha_A = 0.8N$ and a B-homopolymer of length $\alpha_B = 1.5N$. The notation is that of Figure 1. Note the unbinding of the hexagonal phase on the left hand side.

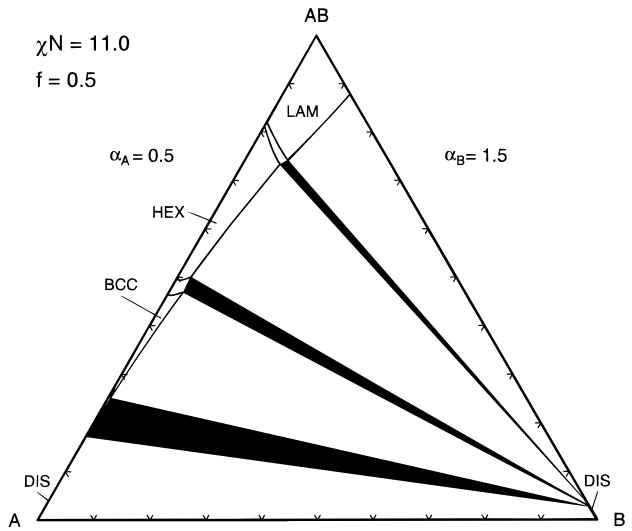

Figure 10. Phase diagram for a symmetric AB-diblock of length N with an A-homopolymer of length $\alpha_A = 1.5N$ and a B-homopolymer of length $\alpha_B = 0.5N$. The notation is that of Figure 1. The unbinding transition is preempted by a first-order transition.

Therefore, its disordering effect is very strong. The B-homopolymer volume fraction in the ordered phases does not exceed 0.15. Note that the coexistence region at the bottom of the phase diagram has vanished; for the given chain lengths, the homopolymers are miscible for $\chi N \leq 12.44$. Also note the continuous transition from the disordered to the lamellar state. This critical point is similar to the point $f = 0.5$, $\chi N = 10.49$ first described by Leibler[2] for the pure diblock melt. It is characterized by a continuously vanishing amplitude of the spatial modulation with a nonzero wavevector.

We now turn to the second sequence, Figures 7−10, in which a B-homopolymer, longer than the diblock ($\alpha_B = 1.5$), is blended with A-homopolymer chains of equal or shorter length. All diagrams are dominated by large coexistence regions between ordered phases, containing less than 0.13 volume fraction of B-homopolymer and an almost pure B-rich disordered phase. On the left hand side, shorter A-homopolymers bring about ordered phases, characterized by more strongly curved internal interfaces, due to the increasing wedge effect of such short homopolymers.

All our results thus far have been obtained for a symmetric diblock and one value of the incompatibility parameter. We now try to extend our findings to moderately asymmetric diblocks and to different temperatures. In Figure 11 we have one example of a system containing an asymmetric diblock, $f = 0.54$, blended with two homopolymers of equal degree of polymerization, $\alpha_A = \alpha_B = 1.0$. The resulting phase diagram is topologically identical to the one in Figure 9. Both are characterized by internal interfaces that have a moderate tendency to curve toward the B-side. In the system in Figure 9, this is brought about by the wedge effect of the homopolymers of unequal length. In that of Figure 11, the diblock layer itself is asymmetric and therefore has a spontaneous curvature. This result and others like it lead us to believe that increasing f and decreasing α_A/α_B have comparable effects on the

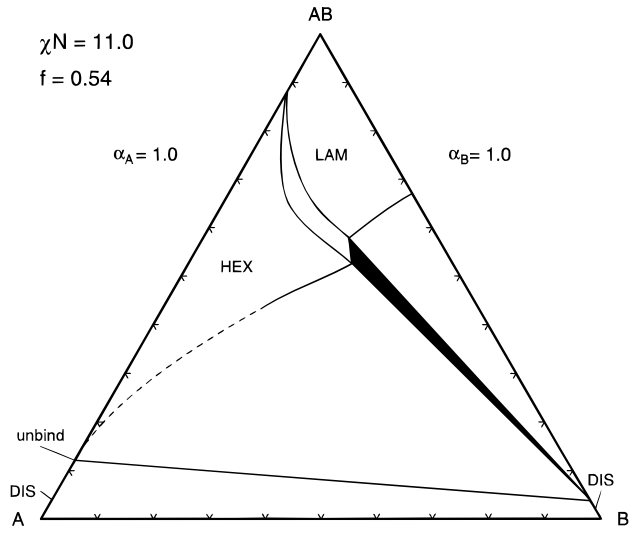

Figure 11. Phase diagram for an asymmetric AB-diblock of N segments, $0.54N$ of which are of type A, blended with corresponding homopolymers with the same number of segments. The notation is that of Figure 1. Note the similarity of this diagram with Figure 9.

overall structure of the phase diagram, at least for roughly symmetric diblock copolymers.

When attempting to extrapolate our results to other temperatures, one can be guided by the following observations. Larger values of χN favor more-strongly segregated configurations. Consequentially, the size of two-phase regions grows with χN. In particular, unbinding transitions may be completely preempted by first-order transitions for values of χN larger than some threshold.[7] On the other hand, at smaller values of χN, one finds more-weakly segregated structures of larger periodicity and a trend toward unbinding of swollen phases. The stability region of ordered phases shrinks as χN decreases. Additional homopolymer with values of α between 0.3 and 1.0, is able to induce microphase ordering, such that blends may be ordered, even if the pure diblock melt is not, and ternary mixtures may be ordered even if the binary blend is not.

Our calculations do not include the effect of fluctuations. Although composition fluctuations are in general strongly suppressed in polymer melts, they are of importance close to a critical point, such as that in Figure 6, and will drive the system to a weakly discontinous transition.[28] However, for most of the parameter space considered here, defects in the spatial ordering will be important. Electron micrographs[12,29] of homopolymer-swollen, ordered microphases reveal a fair degree of disorder, e.g. large amplitude undulations of lamellar phases. This agrees with our result that, for strongly swollen microphases, the minimum of the free energy as a function of the repeat distance becomes extremely shallow. It is likely that the system can lower its free energy by making a first-order transition to disordered micellar or bicontinous phases as suggested in ref 5. Such disordered phases which still contain much structure are not described well by mean-field theory. The occurrence of such a first-order transition, preempting the unbinding transition, would be in accord with the experimental situation in highly swollen amphiphilic systems.[24]

IV. Summary

We summarize our main results for the phase behavior of approximately symmetric diblock copolymers, blended with corresponding homopolymers of varying length.

(1) Homopolymers longer than the diblock ($\alpha > 1$) are expelled from the ordered phases. This is due to the loss of configurational entropy that they would suffer were they confined to the microstructure. Large regions of coexistence, between an ordered phase and a disordered one which contains most of the homopolymer, are formed.

(2) Homopolymers shorter than the diblock enter the brush formed by it, leading to phases characterized by increasing mean curvature of the internal interfaces.

(3) Homopolymers that are slightly shorter or comparable to the diblock ($0.5 \leq \alpha \leq 1.0$) can swell the microphase indefinitely, leading to a complete unbinding transition within mean field theory. We expect thermal fluctuations to destroy a strongly swollen phase and bring about a weak, first-order transition to a disordered phase.

(4) Short homopolymers ($0.25 \leq \alpha \leq 0.5$) swell the microstructure, but because of the substantial entropy they gain upon distributing themselves randomly, they cause the unbinding to be preempted by discontinous transitions. As homopolymers of this length enter cylindrical and spherical structures and relieve stress incurred on the inside of the copolymer layer, they have an ordering effect on the ternary blend.

(5) Very short homopolymers ($\alpha \leq 0.25$) tend to disorder any microphase, since their gain in translational entropy outweighs the enthalpic penalty due to the increased number of A, B-contacts.

(6) For f close to 0.5 and α not very different from 1, increasing f and decreasing α_A/α_B have comparable effects on the overall shape of the phase diagram.

V. Conclusions

We have considered the phase behavior of ternary blends of symmetric and almost symmetric AB-diblock copolymers with corresponding A- and B-homopolymers at all compositions. We find that, depending mainly on the relative chain lengths and the architecture of the diblock, a variety of different behaviors may be observed. Most of these can be explained by "wet" brush/"dry" brush pictures[9,10] and stretching arguments.[11] Our results compare favorably with experimental studies of polymer systems with roughly symmetric diblocks and comparable chain lengths.[12,15,16] Systems with one long and one shorter homopolymer (cf. Figures 1, 9, 10) produce phase diagrams similar to the ones of water/oil/surfactant mixtures (e.g. cf. Figures 37 and 38 of ref 22). Larson[30,31] has modeled the amphiphile in such mixtures by a very short AB-diblock copolymer, and the oil and water by single A- and B-monomers. The model has been studied by extensive Monte Carlo simulations. It is interesting to observe that with $\alpha_A = \alpha_B = 0.25$, the phase diagram obtained[31] with a symmetric diblock is very similar to our Figure 4 with $\alpha_A = \alpha_B = 0.3$, even though Larson considers extremely short chains of N equal to eight. Furthermore, the large extent to which the ordered phases are swollen by homopolymer is comparable in Larson's model to that which we find. This indicates that the disordering effect of fluctuations, present in the simulations but not in our self-consistent field treatment, may not be as great as one would expect. In this connection, it would be desirable to include micellar phases in the mean-field phase diagram and to examine the effect of such structured, yet disordered, phases on the stability of the lyotropic ones.

Acknowledgment. We would like to thank Marcus Müller for fruitful conversations. This work was supported in part by the National Science Foundation under grant DMR9531161.

References and Notes

(1) Matsen, M. W.; Schick, M. *Curr. Opin. Colloid Interface Sci.* **1996**, *1*, 329.
(2) Leibler, L. *Macromolecules* **1980**, *13*, 1602.
(3) Matsen, M. W.; Bates, F. S. *Macromolecules* **1996**, *29*, 1091.
(4) Matsen, M. W. *Phys. Rev. Lett.* **1995**, *74*, 4225.
(5) Matsen, M. W. *Macromolecules* **1995**, *28*, 5765.
(6) Leibler, S.; Lipowsky, R. *Phys. Rev. Lett.* **1987**, *58*, 1796.
(7) Janert, P. K.; Schick, M. *Phys. Rev. E* **1996**, *54*, R33.
(8) De Gennes, P.-G. *Macromolecules* **1980**, *13*, 1069.
(9) Leibler, L. *Macromol. Chem.; Macromol. Symp.* **1988**, *16*, 1.
(10) Leibler, L. *Physica A* **1991**, *172*, 258.
(11) Semenov, A. N. *Macromolecules* **1993**, *26*, 2273.
(12) Inoue, T.; Soen, T.; Hashimoto, T.; Kawai, H. *Macromolecules* **1970**, *3*, 87.
(13) Hashimoto, H.; Fujimura, M.; Hashimoto, T.; Kawai, H. *Macromolecules* **1981**, *14*, 844.
(14) Tanaka, H.; Hasegawa, H.; Hashimoto, T. *Macromolecules* **1991**, *24*, 240.
(15) Löwenhaupt, B.; Hellmann, G. P. *Colloid Polym. Sci.* **1990**, *268*, 885.
(16) Bates, F. S.; Maurer, W.; Lodge, T. P.; Schulz, M. F.; Matsen, M. W.; Almdal, K.; Mortensen, K. *Phys. Rev. Lett.* **1995**, *75*, 4429.
(17) Hu, W.; Koberstein, J. T.; Lingelser, J. P.; Gallot, Y. *Macromolecules* **1995**, *28*, 5209.
(18) Wagner, M.; Wolf, B. A. *Polymer* **1993**, *34*, 1461.
(19) Broseta, D.; Fredrickson, G. H. *J. Chem. Phys.* **1990**, *93*, 2927.
(20) Holyst, R.; Schick, M. *J. Chem. Phys.* **1992**, *96*, 7728.
(21) Banaszak, M.; Whitmore, M. D. *Macromolecules* **1992**, *25*, 249.
(22) Ekwall, P. Composition, Properties and Structure of Liquid Crystalline Phases in Systems of Amphiphilic Compounds In *Advances in Liquid Crystals*; Brown, G. H., Ed.; Academic Press: New York, 1975; Vol. 1.
(23) Tiddy, G. J. T. *Phys. Rep.* **1980**, *57*, 1.
(24) Hecht, E.; Mortensen, K.; Hoffmann, H. *Macromolecules* **1995**, *28*, 5465.
(25) Matsen, M. W.; Schick, M. *Phys. Rev. Lett.* **1994**, *72*, 2660.
(26) Hajduk, D. A.; Harper, P. E.; Gruner, S. M.; Honeker, C. C.; Kim, G.; Thomas, E. L. *Macromolecules* **1994**, *27*, 4063.
(27) Schulz, M. F.; Bates, F. S.; Almdal, K.; Mortensen, K. *Phys. Rev. Lett.* **1994**, *73*, 86.
(28) Fredrickson, G. H.; Helfand, E. *J. Chem. Phys.* **1987**, *87*, 697.
(29) Jeon, K.-J.; Roe, R.-J. *Macromolecules* **1994**, *27*, 2439.
(30) Larson, R. G. *J. Chem. Phys.* **1988**, *89*, 1642; *Ibid.* **1989**, *91*, 2479; *Ibid.* **1992**, *96*, 7904.
(31) Larson, R. G. *J. Phys. II (Fr.)* **1996**, *10*, 1441.

MA961068V